engineering proceedings

MDPI

Proceeding Paper

Design and Construction of Inductive Compensation for Extra-High-Voltage Transmission Line Models of Physical Laboratory of Electric Power Systems †

Anderson Anrrango Delgado, Anghelo Navarrete Cumbal and Jesús Játiva Ibarra *

Escuela Politécnica Nacional, Quito 170143, Ecuador; anderson.anrrango@epn.edu.ec (A.A.D.); anghelo.navarrete@epn.edu.ec (A.N.C.)

* Correspondence: jesus.jativa@epn.edu.ec

† Presented at the XXXII Conference on Electrical and Electronic Engineering, Quito, Ecuador, 12–15 November 2024.

Abstract: The implementation of inductive compensation in the two-scale models of the extra-high-voltage transmission line, without and with transposition, of the Physical Laboratory of Electric Power Systems (PLEPS) is presented. As they have voltages above the normal operating range, for a situation like that of the real 500 kV Coca Codo Sinclair–El Inga lines in Ecuador, the problem was solved by incorporating parallel inductive reactors located at the ends of the lines. The fixed bus compensation used was carried out by means of three-phase inductors in star connection with neutral-to-ground voltage and built-in iron cores with pitches of 50, 75 and 100% of the design capacity.

Keywords: inductive compensation; transmission line scaled models; design and construction

Citation: Anrrango Delgado, A.; Navarrete Cumbal, A.; Játiva Ibarra, J. Design and Construction of Inductive Compensation for Extra-High-Voltage Transmission Line Models of Physical Laboratory of Electric Power Systems. *Eng. Proc.* **2024**, *77*, 31. https://doi.org/10.3390/engproc2024077031

Academic Editor: Walter Vargas

Published: 18 November 2024

1. Introduction

Extra-high-voltage (EHV) transmission lines tend to have overvoltages due to the capacitive effect. To maintain voltage levels within the safety range, one of the solutions used in transmission systems is the injection of reactive power [1]. Transmission lines operating with light or no loads may experience phenomena such as the Ferranti effect. This phenomenon manifests itself when the voltage at the receiving end of the line exceeds the voltage at the sending end, due to the current injected by the capacitance distributed along the line, which causes a voltage increase in the phase with the voltage of the sending end. This increase builds up to the receiving end, resulting in a higher voltage under low- or no-load conditions [2].

To address these challenges, inductive compensation is presented as an effective solution to counteract the adverse effects of line capacitance, absorbing reactive power to keep the receiving-end voltage magnitude close to the rated voltage [3]. This work focuses on the design and construction of scaled inductive compensators, specifically for a model of the Coca Codo Sinclair–San Rafael–El Inga transmission lines, developed at the PLEPS. The steps involved in the process are detailed, ranging from the dimensioning of the compensating power to the operational tests of the system. The work provides a comprehensive view of the calculation of electrical parameters, selection of materials and experimental procedures necessary to validate the technical specifications established during the design.

One of the best ways to understand and learn the electromagnetic phenomena that occur in an electrical system is through a complete physical modeling of its three-phase components, within its size limitations, since it considers asymmetry, electromagnetic couplings and nonlinearities of its elements, as well as the imbalances of its variables, among others. The following statement is relevant in this context: "The complexity of modern power systems is increasing, and thus is requiring of both power engineers and

systems operators a corresponding greater knowledge base upon which to draw form to understand the phenomena occurring in the system, from a systems point of view. This increased understanding cannot be achieved solely through digital modeling but must be complemented by physical modeling" [4].

In the 1970s and 1980s, electromagnetic phenomena were studied in TNA; however, with the development of software, it came to replace it, leaving a void in the research and development of electrical engineering. Some teaching equipment suppliers have three-phase components with many limitations, such as mutual impedance modeling and unloaded and loaded taps on transformers with voltage and angle control. Therefore, a main objective of the Department of Electrical and Electronic Engineering of the National Polytechnic School is to continue developing a physical laboratory based on a scaled power system with four energy sources, two transmission corridors and load centers with residential, commercial and industrial load types as well as a LVDAC-EMS computerized data acquisition system, as shown in Figure 1.

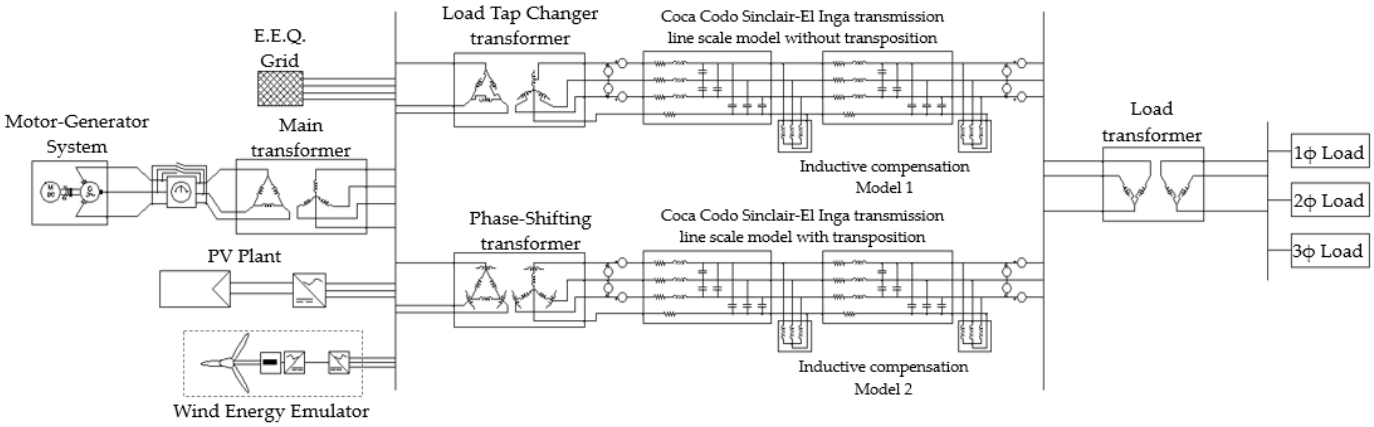

Figure 1. Diagram of the Physical Laboratory of Electrical Power Systems.

Through this research, we seek to demonstrate how the implementation of inductive compensators can mitigate the effects of the Ferranti effect and optimize the performance of transmission lines in a controlled environment with a laboratory voltage level, providing a practical and detailed approach to inductive compensation in EHV transmission systems, such as 500 kV Coca Codo Sinclair–El Inga lines in Ecuador [5].

2. Description of Scale Models of 500 kV Transmission Lines

Inductive compensation is usually placed at the beginning and end of high-voltage transmission lines. The specifications of the actual transmission system and the scale models of the laboratory are presented in Table 1.

Table 1. Specifications of actual transmission line and scale models.

Description	Actual System	Model 1 *	Model 2 **
Base power	1000 MVA	5 kVA	5 kVA
Base voltage	500 kV	220 V	220 V
Base impedance	250 Ω	9.68 Ω	9.68 Ω
Frequency	60 Hz	60 Hz	60 Hz
Resistance	0.015324 Ω/km	0.06708 Ω	0.17947 Ω
Inductive reactance	0.332239 Ω/km	1.55696 Ω	1.52105 Ω
Parallel admittance	4.9857 μS/km	18,835.762 μS	19,049.285 μS

*: Without transposition, **: with transposition.

The scale models were built to represent the Coca Codo Sinclair–San Rafael–El Inga transmission system, which covers approximately 126 km at 500 kV, Figure 2. This system was specifically chosen due to its critical role in the National Interconnected System, as it interconnects the largest hydroelectric plant in Ecuador. One of its complexities is the installation of inductive reactors of 30 MVAr per line at both ends. These reactors are essential for controlling voltage levels and minimizing reactive power imbalances.

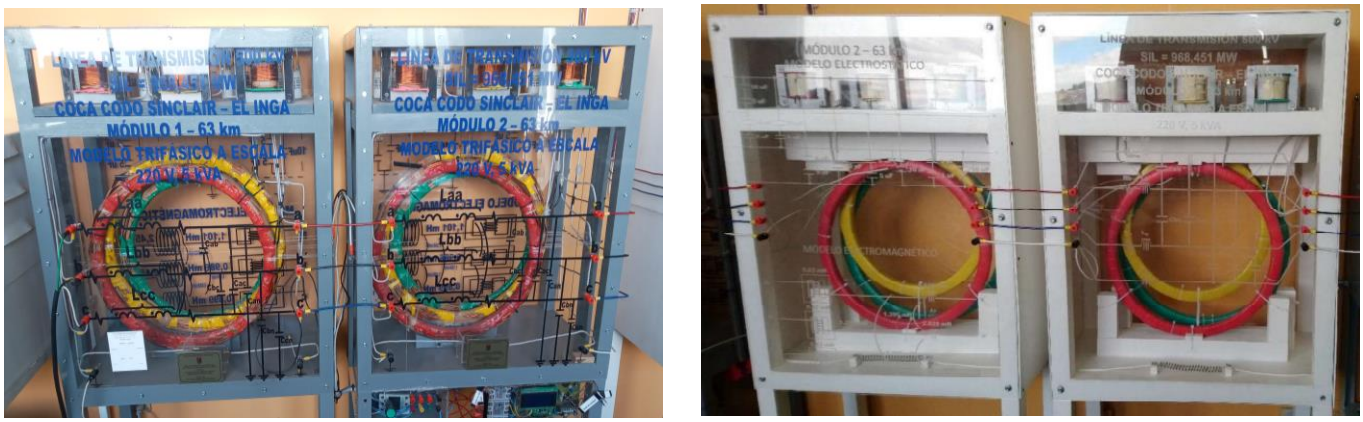

(**a**) (**b**)

Figure 2. Scale models of the Coca Codo Sinclair–San Rafael–El Inga transmission lines. (**a**) Model 1 [6]; (**b**) Model 2 [6], Lii and Lij are self and mutual inductances.

The decision to focus on this system was also due to the need to model real conditions in the transmission of large powers.

To obtain the transmission line models, scaling factors are determined considering the voltage and base power of the real system and PLEPS. To calculate the values in per unit of the actual transmission line, the following base quantities are considered:

$$V_{actual\ base} = 500\ \text{kV and } S_{actual\ base} = 1000\ \text{MVA},$$

while the base quantities compatible with the PLEPS are as follows:

$$V_{model\ base} = 220\ \text{V and } S_{model\ base} = 5\ \text{kVA}.$$

Based on the above relationships, the scaling factors of the transmission line scale model are presented [6,7].

$$Z_{model}\ [\Omega] = \frac{Z_{model\ base}\ [\Omega]}{Z_{actual\ base}\ [\Omega]} Z_{actual}\ [\Omega]$$

$$Z_{model}\ [\Omega] = \frac{(V_{model\ base})^2}{S_{model\ base}} \cdot \frac{S_{actual\ base}}{(V_{actual\ base})^2} \cdot Z_{actual}\ [\Omega]$$

$$Y_{model}\ \left[\Omega^{-1}\right] = \frac{Y_{model\ base}\left[\Omega^{-1}\right]}{Y_{actual\ base}\left[\Omega^{-1}\right]} Y_{real}\ \left[\Omega^{-1}\right]$$

$$Y_{model}\ \left[\Omega^{-1}\right] = \frac{S_{model\ base}}{(V_{model\ base})^2} \cdot \frac{(V_{actual\ base})^2}{S_{actual\ base}} \cdot Y_{actual}\ \left[\Omega^{-1}\right]$$

3. Design and Construction of the Inductive Compensation Coils

The design of inductive compensation coils involves a series of key steps that ensure their effective operation within the scaled transmission models in a laboratory environment.

The flowchart in Figure 3 illustrates the logical sequence followed in the design process from the acquisition of initial parameters to the core construction.

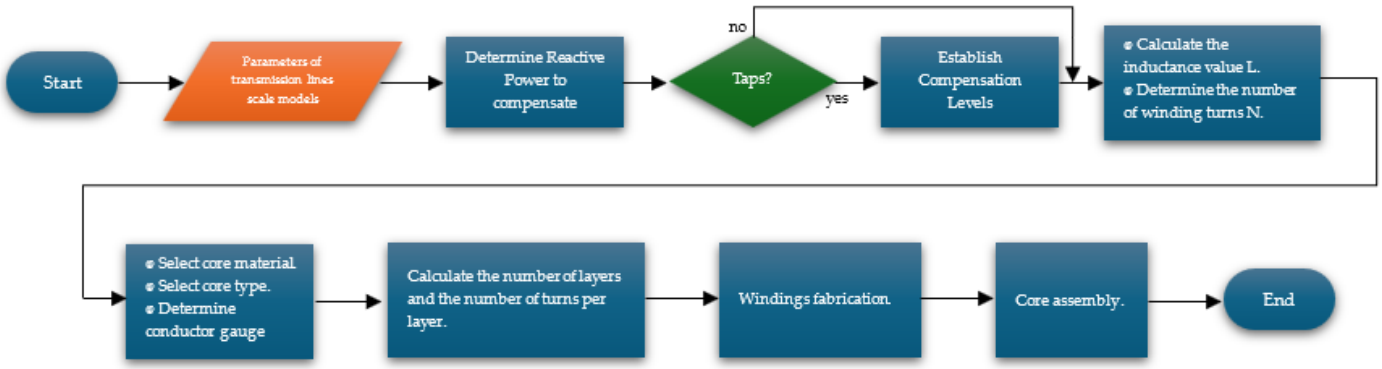

Figure 3. Design flowchart for inductive compensation winding construction.

Determining the reactive power for compensation is one of the crucial steps in the design of inductive compensation coils. This calculation is approached through two methodologies: using the power of the inductive reactors installed in the actual transmission system Coca Codo Sinclair–San Rafael–El Inga and considering the parameters of the scale model of the transmission line. Both methodologies allow compensation adjustments to be made according to the specific characteristics of the power transmitted to the load.

The first approach involves carrying out the process of scaling up the power of the inductive reactors installed in the 500 kV transmission system to the bases of the PLEPS (220 V and 5 kVA) using Equation (1).

$$S_{model} = S_{real}\left(\frac{S_{model\ base}}{S_{actual\ base}}\right) \tag{1}$$

The second approach uses the PLEPS transmission line scale model, as the calculation of the compensation power is based on the electrical parameters of the scale transmission line considering a compensation factor k_c of 70% to avoid the resonance effect of the parallel branches of the line [1,8].

$$k_c = \frac{B_L}{B_C} \tag{2}$$

The calculation of the compensating power is performed per phase according to Equation (3), where $Q_{c/phase}$ is the compensating power per phase, V_{fn} is the nominal neutral-phase voltage of the transmission line, Z_{comp} is the compensating impedance, B_C is the parallel capacitive susceptibility of the transmission line in µS/km, and ℓ is the length of the transmission line in km, Equation (4).

$$Q_{c/phase} = \frac{V_{fn}^2}{Z_{comp}}[\text{VAr}] \tag{3}$$

$$Z_{comp} = \frac{1}{\frac{B_c}{2} * \ell * k_c}[\Omega] \tag{4}$$

The total capacity of the inductive compensation modules is equal to the sum of the compensation power of each phase, Equation (5).

$$Q_c = 3Q_{c/phase}\ [\text{VAr}] \tag{5}$$

In this work, we decided to design and build three-phase modules made up of three inductors with a silicon steel core, which reflects the operation of an inductive compensation reactor in parallel that is installed in the EHV transmission lines. Steel-core inductor banks

allow for reactive power absorption, counteracting the capacitance effects of laboratory transmission line models. Considering the constructive layout of the transmission line scale models, these compensators are placed at the end of each module.

Three levels have been established: 100%, 75% and 50% of the compensation power determined with the methodologies described above. This step, indicated in Figure 3, allows for controlling reactive power according to the needs of the transmission line.

The next step in the flowchart is to calculate the inductance and number of turns. To achieve this, compensating power is used in Equation (6). And with the inductance obtained, the number of turns of the windings of each inductor is calculated with Equation (7) [9].

$$Q_{c/phase} = \frac{V_{fn}^2}{2\pi f L} [\text{VAr}] \tag{6}$$

$$L = \frac{4\pi A_c N^2}{\frac{MPL}{\mu_m}} \times 10^{-7} \text{ [H]} \tag{7}$$

The core of the inductors is constructed using standardized Type EI sheets made of silicon steel, as shown in Figure 3. The EI-type laminate allows easy assembly of the cores, ensuring uniform distribution of magnetic flux and reduction in eddy current losses. At this step of the flowchart, it is necessary to determine the gauge of the conductor. The maximum current flowing through the winding is calculated with Equation (8) and with the use of manufacturers' tables, the appropriate conductor gauge can be chosen.

$$I = \frac{S}{V} \text{ [A]} \tag{8}$$

The calculations obtained in the design are presented in Table 2.

Table 2. Summary of inductive compensator design calculations.

Design Parameter	Symbol	Case 1	Case 2
Single-phase compensation power (100%, 75%, 50%)	$Q_{c/phase}$	50, 37.5, 25 VAr	53.78, 40.34, 26.89 VAr
Core material	-	Silicon steel	Silicon steel
Lamination type	-	EI-125	EI-125
Inductance (100%, 75%, 50%)	L	0.8557, 1.1408, 1.7113 H	0.7957, 1.0609, 1.5914 H
Number of turns (100%, 75%, 50%)	N	304, 351, 430	293, 338, 413
Conductor gauge	-	22 AWG	22 AWG

With the calculations of the design values, the necessary materials for the manufacture of both the windings and the core are obtained. As illustrated in Figure 3, for the construction of the inductors, the wire windings are made in the formworks; for this, a machine with a turn counter is used that guarantees compliance with the number of turns specified in Table 2. For this, it is necessary to determine the number of layers (N_{layers}) and the number of turns (N_b) per layer with Equations (9)–(11), which are also indicated in the flowchart. In these equations, h_b is the height of the coil, G is the internal height of the EI sheets, C is the thickness of the form that isolates the winding from the steel core, f_s is a safety factor, and d_c is the diameter of the conductor. Considering the number of turns of the last compensation level N, Table 3 presents constructive characteristics of the windings.

$$N_b = \frac{h_b}{f_s d_c} \tag{9}$$

$$h_b = G - 2C \tag{10}$$

$$N_{layers} = \frac{N}{N_b} \tag{11}$$

It should be noted that derivations must be made for the winding depending on the number of turns of each compensation level. Once the windings of each of the inductors are available, the core is built by superimposing one sheet after another, completing the process described in Figure 3. If the sheets are placed properly, the edges are aligned correctly; otherwise, it could cause loss of inductance. There are many techniques for the construction of the core, but the most common and the one used in this study was the method that consists of alternating the position of the "E" and the "I"; in this way, maximum permeability is guaranteed.

Table 3. Winding design data.

Construction Parameter	Symbol	Unit	Case 1	Case 2
Total number of turns	N	turns	430	413
Internal height of EI sheets	G	cm	4.8	4.8
Formwork thickness	C	cm	0.1	0.1
Conductor diameter	d_c	cm	0.0644	0.0644
Number of turns per layer	N_b	turns/layer	68	68
Number of layers	N_{layers}	layers	7	6

Figure 4 shows the windings constructed for an inductive compensation module for the transposed line model of the PLEPS.

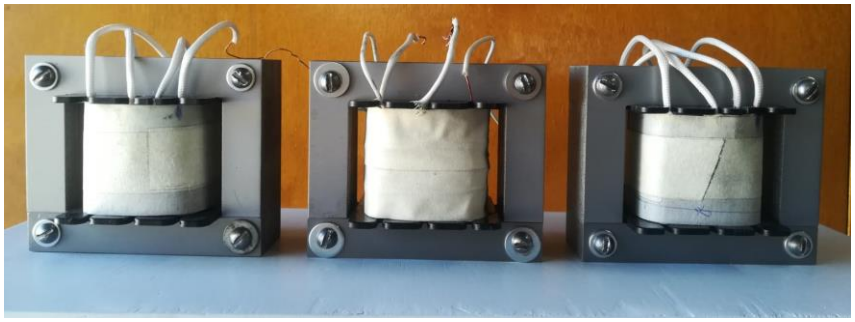

Figure 4. Single-phase inductor bank for an inductive compensation module: 53 VAr, 220 V, 1.5914 H, 1.0609 H and 0.7957 H, respectively.

4. Results

The tests, performed on the inductive compensation modules, are Ferranti effect test, and operational tests with/without loads with each level of compensation, hysteresis curves and saturation curves.

4.1. Hysteresis Curve and Saturation Curve

To validate the design of the compensators, an experimental test was carried out that consisted of assembling an electronic circuit to obtain the hysteresis loop of each of the single-phase inductors built. On the other hand, according to IEC 60076-6 [10], the magnetic characteristic of an inductive reactor is the relationship between the flow links and the current. Since flux bonds cannot be measured directly, it is possible to obtain the saturation curve through an indirect method that consists of obtaining instantaneous measurements of voltage and current at nominal frequency.

The curves obtained from the performance of these tests are those that are presented in Figure 5.

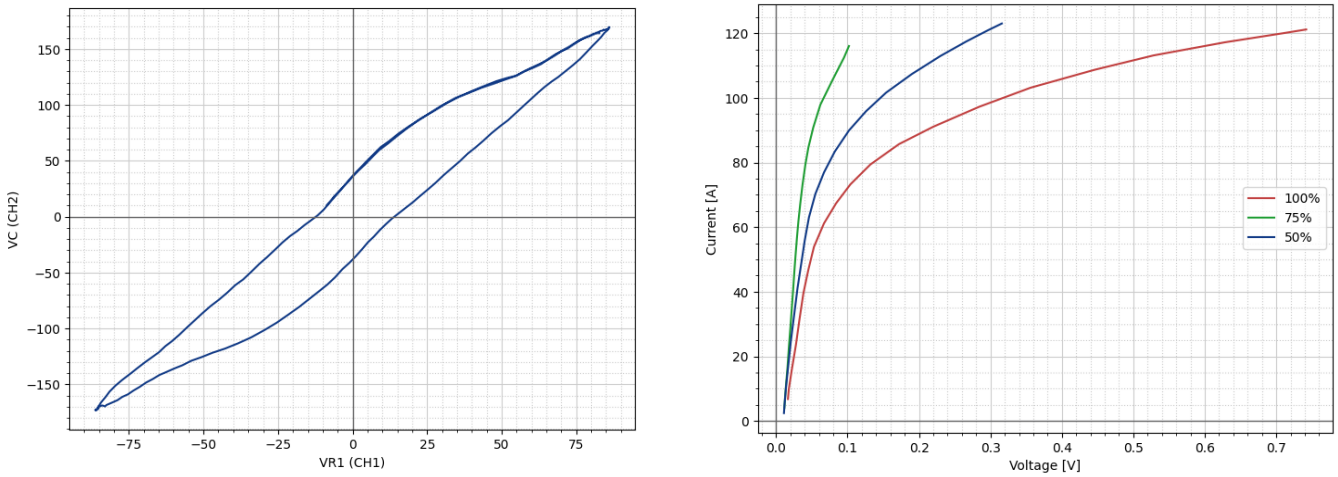

(**a**) (**b**)

Figure 5. Curves obtained for a single-phase inductor. (**a**) Hysteresis curve; (**b**) saturation curve for each compensation level.

4.2. Ferranti Effect

In principle, the no-load and no-compensation test is carried out, which allows the establishment of fundamental reference parameters to demonstrate the operation of the transmission line model before connecting the load and the inductive compensators. In this test, it is possible to observe the Ferranti effect that occurs due to the capacities distributed in the modules of each scale transmission line model. The results of this test are presented in Table 4.

Table 4. Test results without load and without compensation.

	Model 1		**Model 2**	
	Vab	**Vcb**	**Vab**	**Vcb**
Sending bus	217.5 V	217.9 V	220.9 V	221.8 V
Reception bus	222.2 V	221.7 V	224.5 V	226.8 V
Percentage increase	2.16%	1.65%	1.63%	2.25%

In Model 1, it can be observed that the voltage increase between phases A and B is 2.16%, which represents an elevation of 4.6 V in the receiving bus. In Model 2 of the extra-high-voltage line, the capacitive effect causes an increase in the receiving terminals, with 2.25% between phases C and B representing an increase of 5 V.

4.3. No-Load Function Test and with Each Level of Compensation

To analyze the operation of the transmission line models of the laboratory with the inductive compensators connected, measurements were obtained at the sending and receiving terminals of each line model. The results of the test with compensators connected without loads are presented in Table 5.

Considering the tests carried out on the transmission line models without loads attached, Figure 6 shows how the voltage increases in the reception bus vary with the different levels of compensation. In the two initially uncompensated line models, the reception bus shows voltage increases between 3 and 5 V.

Table 5. Test results with no-load inductive compensation.

Compensation Level		Model 1		Model 2	
		Vab	Vcb	Vab	Vcb
50%	Sending bus	219.5 V	219.2 V	223.1 V	224.8 V
	Reception bus	222.7 V	222.5 V	224.2 V	225.9 V
	Percentage increase	1.46%	1.51%	0.493%	0.489%
75%	Sending bus	219.5 V	219.2 V	220.5 V	222.8 V
	Reception bus	222.3 V	222.1 V	221.2 V	223.8 V
	Percentage increase	1.27%	1.32%	0.317%	0.449%
100%	Sending bus	219.5 V	219.2 V	221.1 V	223.7 V
	Reception bus	221.3 V	220.9 V	221.2 V	224.5 V
	Percentage increase	0.82%	0.78%	0.045%	0.358%

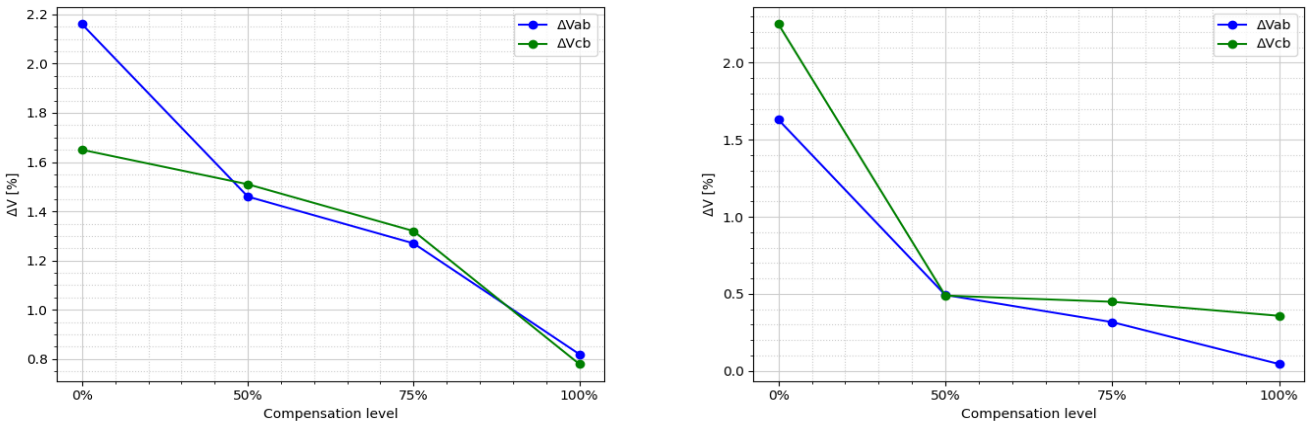

Figure 6. Percentage increase in voltage at the receiving bar for each level of no-load compensation in transmission line-scale models. (**a**) Model 1; (**b**) Model 2.

4.4. Load Test Operation with Each Level of Compensation

The execution of this test allows us to evaluate the behavior of the inductive compensators in the state of operation with loads. At this stage, interactions of the laboratory's transmission line models and reactive compensation to handle the energy demand are observed. In addition, it provides the final validation of the inductive compensation modules, ensuring efficient behavior with all connected components. The results of the test with the compensators connected with loads are presented in Table 6.

Table 6. Test results with 100% inductive and load compensation.

Compensation Level		Model 1		Model 2	
		Vab	Vcb	Vab	Vcb
100%	Sending bus	220.8 V	221.3 V	219.6 V	223.8 V
	Reception bus	221.4 V	221.8 V	219.8 V	224.1 V
	Percentage increase	0.27%	0.23%	0.091%	0.134%

Considering the tests performed on the load and unloaded transmission line models with 100% offset connected, Figure 7 shows the percentage increases for Vab and Vcb in Model 1 and Model 2, with and without loads.

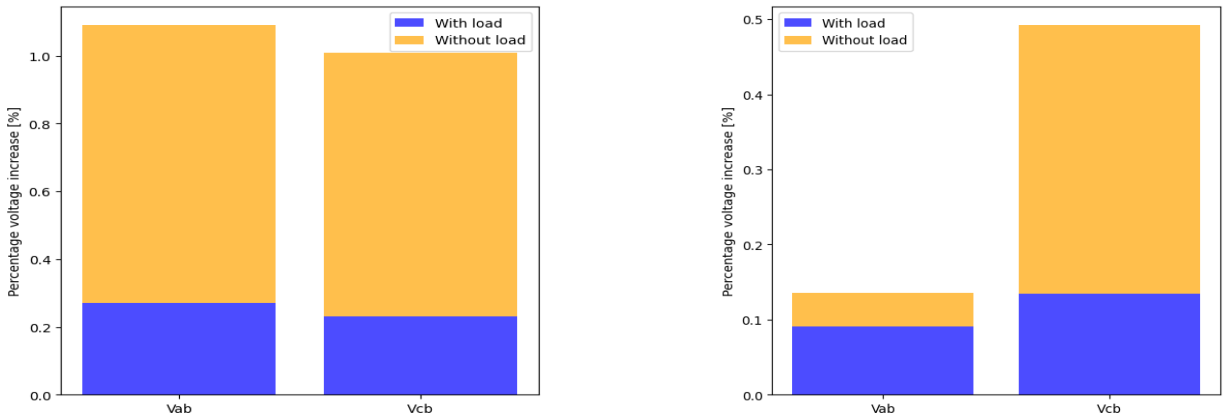

Figure 7. Percentage voltage increase in the reception bus with 100% compensation with and without load in transmission line scale models. (**a**) Model 1; (**b**) Model 2.

The graph corresponding to Model 1 shows the variations in the percentage increase for Vab and Vcb both under load (blue bar) and non-load (orange bar) conditions. The figure reveals that the percentage increase in Vab is greater than in Vcb for both conditions, with significantly higher values in the no-load test compared to the no-load test.

On the other hand, a similar trend is observed in Model 2, although with smaller magnitudes compared to Model 1. This test provides a clear visualization of how load conditions affect percentage increments in both models with their respective inductive compensation connected at 100%.

5. Conclusions

The implementation of the compensation modules proved to be effective in reducing overvoltage at the ends of the transmission line models, which translates into a significant improvement in the quality of electrical variables in the PLEPS.

The effectiveness of the proposed design was verified, where the greater the number of turns of the inductors, the lower the reactive compensating power. The highest number of turns corresponded to 50% compensation with 413 turns, and for 75%, 338 turns were recorded. On the other hand, for 100% compensation, a winding of only 293 turns was required, which corresponded to inductance values of 1.5914 H, 1.0609 H and 0.7957 H, respectively.

The inductive compensation implemented in the PLEPS will serve to carry out research and development in steady-state, dynamic, and transient UHV transmission systems at the undergraduate and graduate levels of electrical engineering.

Author Contributions: Conceptualization, J.J.I.; methodology, A.N.C. and A.A.D.; software, A.N.C.; validation, A.A.D. and A.N.C.; formal analysis, J.J.I.; investigation, A.A.D. and A.N.C.; resources, A.A.D. and A.N.C.; data curation, J.J.I.; writing—original draft preparation, A.A.D.; writing—review and editing, A.A.D. and J.J.I.; supervision, J.J.I.; project administration, J.J.I.; funding acquisition, A.A.D. and A.N.C. All authors have read and agreed to the published version of the manuscript.

Funding: This research received no external funding.

Institutional Review Board Statement: Not applicable.

Informed Consent Statement: Not applicable.

Data Availability Statement: Data are contained within the article.

Conflicts of Interest: The authors declare no conflicts of interest.

References

1. Kundur, P. *Power System Stability and Control*; McGraw-Hill: New York, NY, USA, 1993.
2. Foqha, T.; Alsadi, S.; Refaat, S.S.; Abdulmawjood, K. Experimental Validation of a Mitigation Method of Ferranti Effect in Transmission Line. *IEEE Access* **2023**, *11*, 15878–15895. [CrossRef]
3. Mondal, D.; Chakrabarti, A.; Sengupta, A. *Power System Small Signal Stability Analysis and Control*, 2nd ed.; Elsevier: London, UK; Academic Press: Cambridge, MA, USA, 2020.
4. Domijan, A. *Overall Conceptual Development, Planning, and Design Aspects of an Electric Power System Laboratory with an Energy Management System Control Center*; The University of Texas at Arlington: Arlington, TX, USA, 1986.
5. *Plan Maestro de Electrificación 2013-2022, Perspectiva y Expansión del Sistema Eléctrico Ecuatoriano*; Consejo Nacional de Electricidad CONELEC: Quito, Ecuador, 2013.
6. Pagalo, D.; Quintana, E. *Diseño y Construcción de un Transformador Trifásico para Control de Ángulo y un Modelo a Escala de Línea de Transmisión de 500 kV para el Laboratorio de Sistemas Eléctricos de Potencia*; Trabajo de Titulación, Escuela Politécnica Nacional: Quito, Ecuador, 2019.
7. Ramos, M.C.; Tupiza, S.R. *Diseño y Construcción de un Modelo a Escala de la Línea De Transmisión de 500 kV Coca Codo Sinclair-El Inga para el Laboratorio de Sistemas Eléctricos de Potencia*; Trabajo de Titulación, Escuela Politécnica Nacional: Quito, Ecuador, 2018.
8. Yonggao, Z.; Wanqing, L.; Yanli, G. Research on reactive compensation in ultra-high voltage power grid using shunt reactors. In Proceedings of the 2016 IEEE 11th Conference on Industrial Electronics and Applications (ICIEA), Hefei, China, 5–7 June 2016.
9. McLyman, C.W.T. *Transformer and Inductor Design Handbook*, 4th ed.; CRC Press: Boca Raton, FL, USA, 2011.
10. *IEC 60076-6*; Power Transformers—Part 6: Reactors. Available online: https://www.saiglobal.com/PDFTemp/Previews/OSH/iec/iec60000/60000/iec60076-6%7Bed1.0%7Db.pdf (accessed on 30 September 2024).